

## Low-energy $\pi$ NN system

Vadim Baru<sup>1,2,a</sup>

<sup>1</sup> Forschungszentrum Jülich, Institut für Kernphysik (Theorie) and Jülich Center for Hadron Physics, D-52425 Jülich, Germany

<sup>2</sup> Institute for Theoretical and Experimental Physics, B. Chermushkinskaya 25, 117218 Moscow, Russia

**Abstract.** The reaction  $NN \rightarrow NN\pi$  is studied at low energies within chiral perturbation theory (ChPT). Special emphasis is put on p-wave pion production in different channels of  $NN \rightarrow NN\pi$  and Charge Symmetry Breaking (CSB) effects in  $pn \rightarrow d\pi^0$  recently measured at TRIUMF. A very good agreement of the p-wave amplitudes with experimental observables demonstrates the applicability of ChPT to these reactions regardless the large momentum transfer. The results of a complete calculation of CSB effects at leading order are presented. Based on this calculation we extract the strong contribution to the neutron-proton mass difference.

### 1 Introduction

Chiral perturbation theory (ChPT) is a modern framework to systematically investigate low-energy hadronic reactions [1,2]. ChPT is based on the most general effective Lagrangian consistent with the symmetries of QCD. In this approach the pion is associated with the lightest Goldstone boson of the spontaneously broken approximate chiral SU(2) symmetry of QCD. It is a consequence of the Goldstone theorem that bosons with vanishing momenta do not interact with hadrons in the chiral limit, i.e. in the limit of vanishing light-quark masses ( $m_u = m_d = 0$ ). Therefore once we are interested in the hadronic process at low energies sufficiently close to this limit the scale induced by the boson momentum  $q$  is normally of the order of the pion mass ( $M_\pi^2 \sim m_u + m_d$ ) and it is much smaller than the typical hadronic scale of the order of  $\Lambda_\chi \sim m_N \sim 1$  GeV where  $m_N$  is the nucleon mass. Thus the low-energy hadronic reactions can be studied perturbatively, order by order, based on the expansion parameter  $\chi \sim q/\Lambda_\chi$  with a controlled error estimate. The framework has been successfully applied to study, in particular,  $\pi\pi$  [3] and  $\pi N$  [4] scattering observables as well as nuclear forces [5]. Furthermore, the approach was extended by Weinberg [6] to the low-momentum transfer pion reactions on few nucleon systems. He proposed the so-called hybrid approach which consists of two steps:

1. The pion transition (production) operators are perturbative. Thus, they can be calculated systematically using ChPT. At any given order they should consist of all possible irreducible graphs.
2. The transition operators have to be convoluted with the non-perturbative  $NN$  wave functions.

<sup>a</sup> e-mail: v.baru@fz-juelich.de

Many low-energy reactions involving pions, e.g.  $\pi d \rightarrow \pi d$  [7–9] and  $\pi He^3 \rightarrow \pi He^3$  [10],  $\pi d \rightarrow \gamma NN$  [11,12],  $\gamma d \rightarrow \pi NN$  [13,14], as well as  $\gamma d \rightarrow \pi^0 d$  [15,16] have been successfully investigated within the hybrid approach, using Weinberg's power counting.

However, an application of the scheme naively to pion production in NN collisions failed completely [17,18]. Indeed, the inclusion of the tree level corrections at next-to-leading-order (NLO) made the discrepancy between theory and data even stronger both for neutral and charged pion production [17,18]. Moreover, it was even shown that the corrections at next-to-next-to-leading-order (N<sup>2</sup>LO) are larger than those at NLO which basically demonstrated the non-applicability of Weinberg's power counting to this type of reactions (see also Ref. [19] where it was pointed out that the naive power counting using the heavy baryon formalism is not applicable above the pion production threshold).

Progress was made in Refs. [20,21] where it was advocated that the initial nucleon momentum in threshold kinematics provides a new "small" scale in the problem, namely,  $p \simeq \sqrt{m_N M_\pi} \simeq 360$  MeV ( $\chi \simeq p/m_N \simeq \sqrt{M_\pi/m_N}$ ). The proper way to include this scale in the power counting was presented in Ref. [22] and implemented in Ref. [23], see Ref. [24] for a review article. As a consequence, the hierarchy of diagrams changes in the modified power counting scheme of Ref. [22], and some loops start to contribute already at NLO for s-wave pion production. The convergence of the chiral expansion in the modified power counting was studied in Ref. [25] via s-wave pion production in  $pp \rightarrow d\pi^+$ . It was found that the total cross section is described nicely already at leading order (LO) and that all

corrections at NLO are negligible<sup>1</sup>. On the other hand, the theoretical uncertainty of the NLO calculation is relatively large ( $\sim M_\pi/m_N \simeq 15\%$  for the amplitude) and the calculation of loops at N<sup>2</sup>LO is necessary to further explore the convergence of the chiral expansion, see Ref. [26] for the first calculation of this kind. Also at N<sup>2</sup>LO two new LECs start to contribute: one in the  ${}^3P_0 \rightarrow {}^1S_0$  partial wave ( $pp \rightarrow pp\pi^0$  channel) and one in  ${}^3P_1 \rightarrow {}^3S_1$  ( $pp \rightarrow d\pi^+$  channel). Therefore it would be very educating to see if these LECs are of natural size or not as an additional test of the consistency of the scheme.

On the other hand, a very good test of the applicability of ChPT to the reactions with large-momentum transfer is provided by the study of p-wave pion production, for in this case loops (that are technically much more involved) start to contribute only at N<sup>3</sup>LO. Therefore a calculation of tree level diagrams up to (and including) N<sup>2</sup>LO is relatively simple and useful. For p-wave pions the calculation at LO and NLO does not involve any free parameters whereas at N<sup>2</sup>LO there is only one LEC contributing to different channels of  $NN \rightarrow NN\pi$ : it appears in  ${}^1S_0 \rightarrow {}^3S_1$  for  $pp \rightarrow d\pi^+$  and  $pp \rightarrow pn\pi^+$  and in  $({}^3S_1 - {}^3D_1) \rightarrow {}^1S_0$  for  $pn \rightarrow pp\pi^-$ . We discuss the status of p-wave pion production in Sec. 2, see also Ref.[27] for more details. It was found, in particular, that the net contribution of diagrams at N<sup>2</sup>LO is indeed of natural size. Moreover, it turned out to be possible to describe data in different channels of  $NN \rightarrow NN\pi$  with the same value of the LEC. The goal of this contact interaction is to parameterize the short range physics and to absorb the sensitivity to the NN interaction used. Thus, it necessarily depends on the form on the NN wave functions and the method of regularization of the loop integrals. Since NN interaction in the same partial wave contributes in different channels of  $NN\pi$  in very different kinematical regimes (e.g. the pp-system in the  ${}^1S_0$  partial wave enters at very low relative momenta in the regime of the final state interaction (FSI) which is the case of  $\pi^-$  production whereas for  $\pi^+$  production it contributes to the initial state interaction (ISI) at relatively large momenta) the quantitative agreement in the magnitude for the LEC provides a consistency check of the scheme.

The status of the theory for pion production in the isospin conserving case allows one to address charge symmetry breaking (CSB) effects recently observed experimentally in  $pn \rightarrow d\pi^0$  [28]. It was first argued in Ref. [29] that CSB effects in the reaction  $pn \rightarrow d\pi^0$  provide access to the strong part of the neutron-proton mass difference (due to the quark mass difference) which is the fundamental quantity of QCD. In addition, there is a contribution due to the electromagnetic interactions [30], i.e.  $\delta m_N = m_n - m_p = \delta m_N^{\text{str}} + \delta m_N^{\text{em}}$ . As a result of the chiral structure of the QCD Lagrangian, the strength of the rescattering operator contributing to  $pn \rightarrow d\pi^0$  is proportional to a different combination of  $\delta m_N^{\text{str}}$  and  $\delta m_N^{\text{em}}$  [29]. Therefore studying the reaction  $pn \rightarrow d\pi^0$  allows one to determine  $\delta m_N^{\text{str}}$  and  $\delta m_N^{\text{em}}$  independently Ref. [29], ( see also Ref. [31,32] for related

works). In Sec. 3 we will present the results of a complete calculation of CSB effects at LO [33]. We will also compare our results with those of Refs. [29,34].

## 2 $NN \rightarrow NN\pi$ with p-wave pions

In this section we discuss p-wave pion production in the reaction channels  $pp \rightarrow pn\pi^+$ ,  $pp \rightarrow d\pi^+$  and  $pn \rightarrow pp\pi^-$ . The main goal of the study is to demonstrate that the experimental observables in all these channels can be simultaneously described by adjusting only one LEC representing a  $(\bar{N}N)^2\pi$  contact term. Since this contact term is operative when the nucleons (both initial and final) are in  $S$ -wave we will concentrate on observables where the final  $NN$  system is in an  $S$ -wave only. Note also that this contact term does not contribute to  $pp \rightarrow pp\pi^0$  where a p-wave pion can be produced only in combination with the final P-wave NN-pair. That is why this channel is disregarded in our investigation.

As briefly sketched in the Introduction up to N<sup>2</sup>LO there are only tree level diagrams, as given in Fig. 1, contributing to p-wave pion production. In particular, at NNLO there are subleading rescattering and direct pion production operators as well as the  $(\bar{N}N)^2\pi$  contact term. Notice that it is the same contact term that also contributes to the three-nucleon force [22,35], to the processes  $\gamma d \rightarrow \pi NN$  [13,14] and  $\pi d \rightarrow \gamma NN$  [11,12] as well as to weak reactions such as, e.g., tritium beta decay and proton-proton ( $pp$ ) fusion [36,37]. Therefore it provides a connection between different low-energy reactions. Furthermore, this operator appears in the above reactions in very different kinematics, ranging from very low energies for both incoming and outgoing  $NN$  pairs in proton-deuteron scattering and the weak reactions up to relatively high initial energies for the  $NN$  induced pion production. As a part of this connection in Ref. [38] it was shown that both the  ${}^3\text{H}$  and  ${}^3\text{He}$  binding energies and the triton  $\beta$ -decay can be described with the same contact term. However, an apparent discrepancy between the strength of the contact term needed in  $pp \rightarrow pn\pi^+$  and in  $pp \rightarrow de^+v_e$  was reported in Ref. [39]. If the latter observation were true, it would question the applicability of chiral EFT to the reactions  $NN \rightarrow NN\pi$ . To better understand the discrepancy reported in Ref. [39], in the recent paper [27] we simultaneously analyzed different pion production channels. In particular, we calculated the p-wave amplitudes for the reactions  $pn \rightarrow pp\pi^-$ ,  $pp \rightarrow pn\pi^+$ , and  $pp \rightarrow d\pi^+$ . Note that even in the different channels of the production process the contact term connects NN wave functions in entirely different kinematic regimes. For the first channel p-wave pion is produced along with the slowly moving protons in the  ${}^1S_0$  final state whereas for the other two channels the  ${}^1S_0$   $pp$  state is to be evaluated at the relatively large initial momentum, see Fig. 2 for illustration. As seen from this Figure, the contribution of the contact operator scales as the product of the NN wave functions at the origin. Each of these wave functions, in turn, may be represented by the inverse of the corresponding Jost function [40]. The reason why it is expected to be possible that the same contact term can be

<sup>1</sup> Based on this study in Refs. [9] the dispersive corrections to the pion-deuteron scattering length were first calculated systematically, i.e. within ChPT.

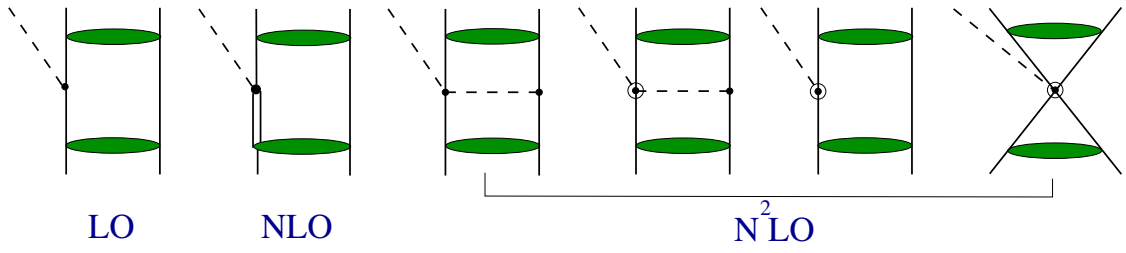


Fig. 1. Diagrams contributing to p-wave pion production up to  $N^2LO$ .

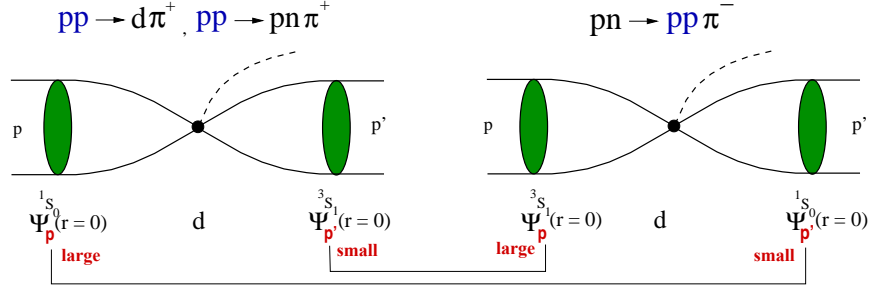


Fig. 2. Illustration of the contact term (labeled as  $d$ ) contribution in different channels of  $NN \rightarrow NN\pi$ . Labels "small" and "large" indicate that the  $NN$  wave functions in the same partial wave contribute in different  $NN$  channels in different kinematic regimes.

used in all reactions mentioned above is that the energy dependence of the Jost function is fixed by the onshell  $NN$  data (up to a polynomial which is expected to be a smooth function of the momenta) and is therefore model independent. Specifically, the  $NN$  wave functions at the origin can be represented as an integral over the relevant phase shifts  $\delta_{NN}$  by means of the so-called Omnès function [41] (see also the discussion in Ref. [42])

$$\begin{aligned} \Psi_q(r=0) &= 1 + m_N \int_0^\infty d^3 q' \frac{T(q', q, q)}{q^2 - q'^2 + i0} \\ &= C \exp \left\{ \frac{1}{\pi} \int_{4m_N^2}^\infty ds' \frac{\delta_{NN}(s')}{s' - s(q) + i0} \right\}, \end{aligned} \quad (1)$$

where  $T$  is the  $NN$  T-matrix,  $s(q) \simeq (2m_N + q^2/m_N)^2$  for the nonrelativistic nucleons and  $C$  is a model-dependent constant (up to higher order terms in  $q/m_N$ ). Thus the whole momentum dependence of the contact term contribution is model-independent, since it is fully determined by the product of two Omnès functions for the  $^1S_0$  and  $^3S_1$  partial waves whereas the product of the constants  $C_{1S_0}$  and  $C_{3S_1}$  can be absorbed in the strength of the contact term (LEC  $d$ ) for all channels of  $NN \rightarrow NN\pi$ . The details of the calculation and explicit expressions for the diagrams can be found in Ref. [27]. Since the value of the LEC  $d$  depends strongly on the type of  $NN$  interaction and the regularization scheme it is not possible to compare directly the values of  $d$  as found in different calculations. What can be done, however, is the comparison of the results on the level of observables. Following this logic we adjusted the value of  $d$  in such a way to get the best simultaneous qualitative description of all channels of  $NN\pi$ . In Fig.3 we compare our results for various values of  $d$  with the experimental data

for the analyzing power for the reaction  $pp \rightarrow d\pi^+$ . We find that the data prefer a positive value of  $d$  of about 3. A similar pattern can be observed in the reaction  $pn \rightarrow pp\pi^-$  as illustrated in Fig. 4. Again the data show a clear preference of the positive value for LEC  $d$  – our fit resulted in  $d = 3$  for the best value. This channel, however, has been measured at TRIUMF at relatively large excess energy<sup>2</sup> ( $\eta = 0.66$ ) where the conclusion may be spoiled due to the onset of pion d-waves. Fortunately, a new measurement for the same observables at lower energies is currently on-going at COSY [48] which will soon allow a quantitative extraction of the value of the LEC  $d$ . We now turn to the reaction  $pp \rightarrow pn\pi^+$  – this channel was used in the analysis of Ref.[39]. The reaction  $pp \rightarrow pn\pi^+$  should have, in principle, the same information on the LEC  $d$  as contained in the deuteron channel. However, it is much more difficult to extract the pertinent information unambiguously from this reaction. In particular, the final  $NN$ -system might be not only in  $S$ - but also in  $P$ -wave both for isospin-zero and for isospin-one  $NN$  states. At the energies considered in the experimental investigation,  $\eta = 0.22, 0.42,$  and  $0.5$ , the  $Pp$  amplitudes may contribute significantly [52–54]. In the current study these states are disregarded. The results of our calculation for the magnitude  $A_2$  are given<sup>3</sup> in the left panel of Fig. 6. One finds again that the positive LEC  $d \simeq 3$  seems to be preferred. Thus we conclude that all reaction channels of  $NN \rightarrow NN\pi$  can be described simultaneously with the same value of the LEC  $d$ . Coming back to the problem raised in Ref. [39] it should be pointed out that the results of this work were not compared

<sup>2</sup> Traditionally the energy for pion production reactions is given in terms of  $\eta$ , the pion momentum in units of the pion mass

<sup>3</sup> The coefficients  $A_i$  are related to the unpolarized differential cross section via  $\frac{d\sigma}{d\Omega} = A_0 + A_2 P_2(x)$ , with  $P_2(x)$  being the second Legendre polynomial

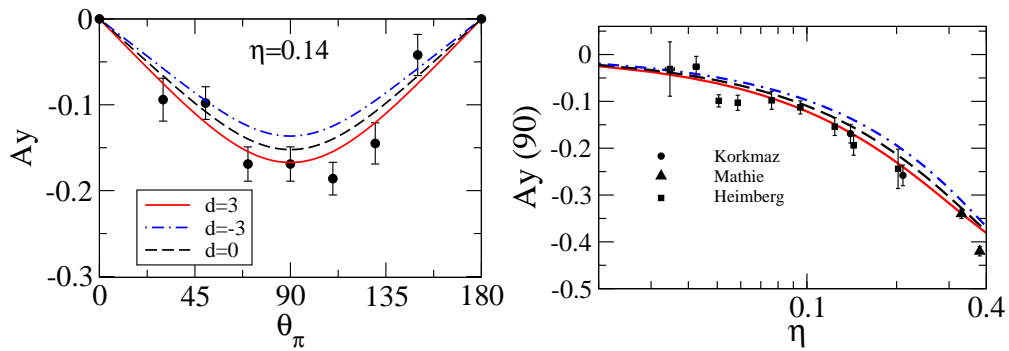


**Fig. 3.** Results for the analyzing power at  $\eta=0.14$  (left panel) and the analyzing power at 90 degrees (right panel) for the reaction  $pp \rightarrow d\pi^+$  for different values of the LEC  $d$  (in units  $1/(f_\pi^2 M_N)$ ) of the  $(\bar{N}N)^2\pi$  contact operator. Shown are  $d = 3$  (red solid line),  $d = 0$  (black dashed line), and  $d = -3$  (blue dot-dashed line). The data are from Refs. [43–47].

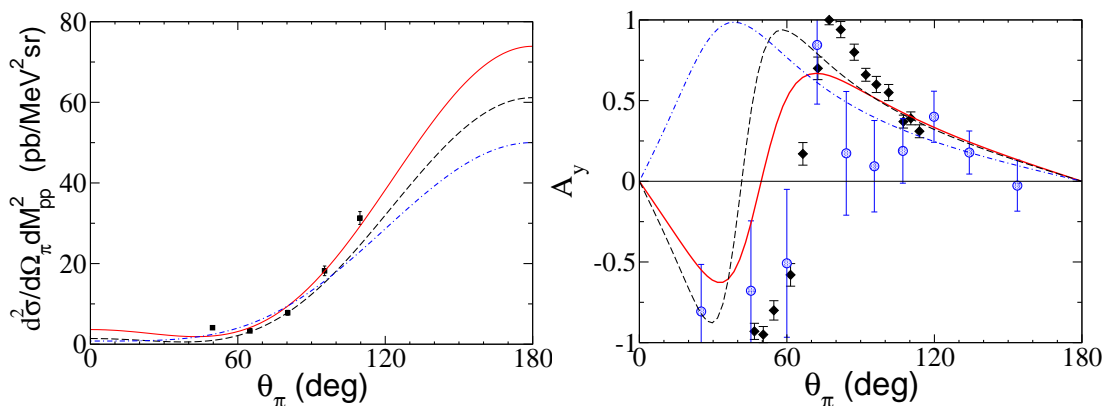


**Fig. 4.** Results for  $d^2\sigma/d\Omega_\pi dM_{pp}^2$  (left panel) and  $A_y$  (right panel) for  $pn \rightarrow pp(^1S_0)\pi^-$ . Shown are the results for  $d = 3$  (red solid line),  $d = 0$  (black dashed line) and  $d = -3$  (blue dot-dashed line). The data are from TRIUMF [49,50] (black squares) and from PSI [51] (blue circles).

directly to the observables in  $pp \rightarrow pn\pi^+$ . Instead, they were compared to the results of the partial wave analysis (PWA) performed in Ref.[55], as demonstrated in the right panel of Fig. 6. It is based on this discrepancy between data and theory it was concluded in Ref.[39] about the failure of simultaneous description of the weak processes and  $NN \rightarrow NN\pi$ . However, the partial wave analysis of Ref.[55] seems to be not correct. Here we refer the interested reader to Ref.[27] where the drawbacks of this PWA are discussed in detail. To illustrate the problems of the PWA in the right panel of Fig. 6 we also show the results of our calculation for the relevant partial wave  $a_0$  which corresponds to the transition  $^1S_0 \rightarrow ^3S_1 p$  where the contact term acts. Clearly, although all data presented in Ref. [55] are in a good agreement with our calculation (see left panel in Fig. 6 and also Ref.[27] for more details), the partial wave amplitude  $a_0$  is not at all described. Thus, we think that the problem with the simultaneous description of  $pp \rightarrow de^+v_e$  and  $pp \rightarrow pn\pi^+$ , raised in Ref.[39], is due to the drawbacks of the partial wave analysis of Ref.[55]. In addition, we think that there is also some technical problem in the work of Ref. [39]: as was discussed above, as long as different phase-equivalent  $NN$  interactions are used, it

should be possible to absorb the model dependence of the calculation in a single counter term available in the problem. However, this argument should be operative only if all  $NN$  amplitudes relevant for the study are calculated consistently from the same  $NN$  potential which was fitted to data. But it is not really what was done in Ref. [39]. The p-wave pion production amplitudes get an important contribution from the diagram at NLO that involves the excitation of the  $\Delta$  isobar in the intermediate state. Therefore the transition  $NN \rightarrow N\Delta$  is relevant for the study. However, the  $NN$  models used in Ref. [39] do not contain the  $N\Delta$  channel explicitly. Rather the contribution from the  $\Delta$  isobar excitation is added on top (independently) of the employed  $NN$  interactions. Thus, it is quite possible that the utilized  $NN \rightarrow N\Delta$  transition potential is too strong – see also a recent study [34] where exactly this problem led to a strong overestimation of the differential cross section in  $NN \rightarrow d\pi$ . Specifically, the  $NN \rightarrow N\Delta$  transition is not constrained by the empirical  $NN$  phase shifts as it is the case when considering the  $NN$  and  $N\Delta$  amplitudes consistently within a coupled-channel (Lippmann-Schwinger-like) scattering equation [56,57]. To avoid this problem, in this work we employ the coupled-channel  $NN$  model of

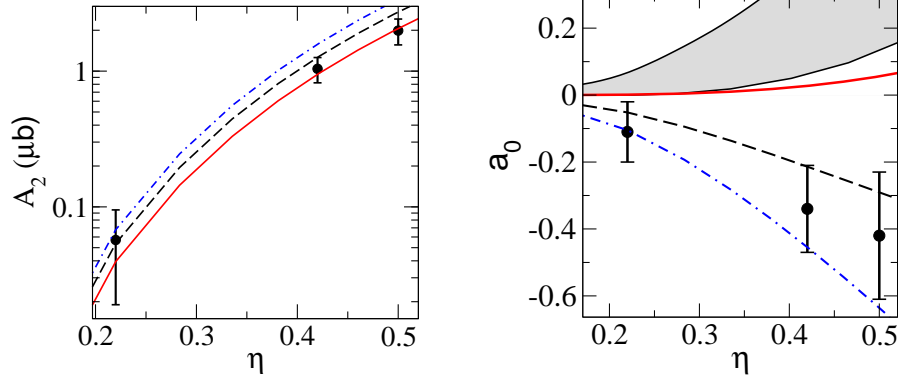


**Fig. 5.** Results for the magnitude  $A_2$  (left panel) and the partial wave amplitude  $a_0(\sqrt{\mu b})$  representing the relevant transition  $^1S_0 \rightarrow ^3S_1 p$  (right panel) for  $pp \rightarrow pn\pi^+$  for different values of the LEC  $d$ . The notation is the same as in Fig. 3, gray band corresponds to the results of Ref. [39]. The data are from Ref. [55].

Ref. [57] which involves the  $NN \rightarrow N\Delta$  transition potential.

### 3 Charge symmetry breaking in $pn \rightarrow d\pi^0$ at leading order.

In this section we discuss how CSB effects evaluated at LO can be used to extract the strong contribution to the neutron-proton mass difference induced by the quark mass difference.

#### 3.1 Observables

The differential cross section of the reaction  $pn \rightarrow d\pi^0$  can be expanded into a series of Legendre polynomials  $P_i(\cos \theta)$ . In the near threshold region only the first terms are relevant

$$\frac{d\sigma}{d\Omega}(\theta) = A_0 + A_1 P_1(\cos \theta) + \dots, \quad (2)$$

where  $\theta$  is the angle between the incident proton and the pion produced and the  $A_i$  are functions depending on the different partial wave amplitudes. Due to CSB effects the differential cross section is not symmetric with respect to an interchange of proton and neutron, i.e.

$$\frac{d\sigma}{d\Omega}(\theta) \neq \frac{d\sigma}{d\Omega}(\pi - \theta)$$

and thus  $A_1$  is non-vanishing. The forward-backward asymmetry is defined as

$$A_{fb} = \frac{\int_0^{\pi/2} \left[ \frac{d\sigma}{d\Omega}(\theta) - \frac{d\sigma}{d\Omega}(\pi - \theta) \right] \sin\theta d\theta}{\int_0^{\pi/2} \left[ \frac{d\sigma}{d\Omega}(\theta) + \frac{d\sigma}{d\Omega}(\pi - \theta) \right] \sin\theta d\theta} = \frac{A_1}{2A_0}, \quad (3)$$

where we used Eq. (2) in the last equality. The experiment at TRIUMF was done very close to threshold at  $T_{\text{lab}} =$

279.5 MeV, which is equivalent to an excess energy of about 2 MeV or  $\eta = 0.17$ . At this energy the total cross section  $\sigma = 4\pi A_0$  is dominated by the isospin conserving  $s$ -wave pion production amplitude. At present, this quantity is known theoretically (see Ref.[25,58]) only up-to-and-including terms at NLO which implies a theoretical uncertainty of the order of 30% for the cross section. Moreover, as already sketched in the introduction, at  $N^2\text{LO}$  there is one contact term in this channel the strength of which will be anyway adjusted to achieve an agreement with the experimental data<sup>4</sup>. Therefore, to minimize the uncertainty of the current study, we use the experimental value for  $\sigma(nn \rightarrow d\pi^-) = 252_{-11}^{+5} \cdot \eta$  [μb] extracted with very high accuracy from the lifetime of the pionic deuterium atom measured at PSI [59]. Note that there is a wealth of experimental data for the total cross section measured "in flight" (i.e. in the scattering experiments). Those measurements, however, suffer from a normalization uncertainty whereas the only measurement at rest, as performed at PSI, is free of this problem. To convert this number to the reaction of interest here we may use isospin symmetry which gives  $\sigma(pn \rightarrow d\pi^0) = \sigma(nn \rightarrow d\pi^-)/2$ . Isospin violating effects in this relation are to be expected of natural size and thus will not further be considered. In addition, we include in  $A_0$  also the contribution from the  $p$ -wave production amplitudes which is about 10% of the total cross section at the energy considered. Here we take the results of the  $N^2\text{LO}$  calculation of Ref. [27] discussed in Sec.2. Thus, we get in total  $A_0 = 10.0_{-0.4}^{+0.2} \cdot \eta + (47.8 \pm 5.7) \cdot \eta^3$  [μb].

At the energies we consider here, the function  $A_1$  depends on the interference of either an isospin conserving (IC)  $p$ -wave and an isospin violating (IV)  $s$ -wave amplitude or of an IV  $p$ -wave with an IC  $s$ -wave. However, only the former piece contributes at leading order. Thus, to the order we are working, the relevant transition amplitudes are

$$\mathcal{M}_{pn \rightarrow d\pi^0}^{\text{IC},p} = M_1^{\text{IC},p} \mathcal{I}(\hat{k}_\pi \varepsilon) + M_2^{\text{IC},p} \mathcal{I}[(\hat{p} \hat{k}_\pi)(\hat{p} \varepsilon) - \frac{1}{3}(\hat{k}_\pi \varepsilon)],$$

<sup>4</sup> The question whether this LEC is natural or not is clearly important to understand how the chiral expansion converges.

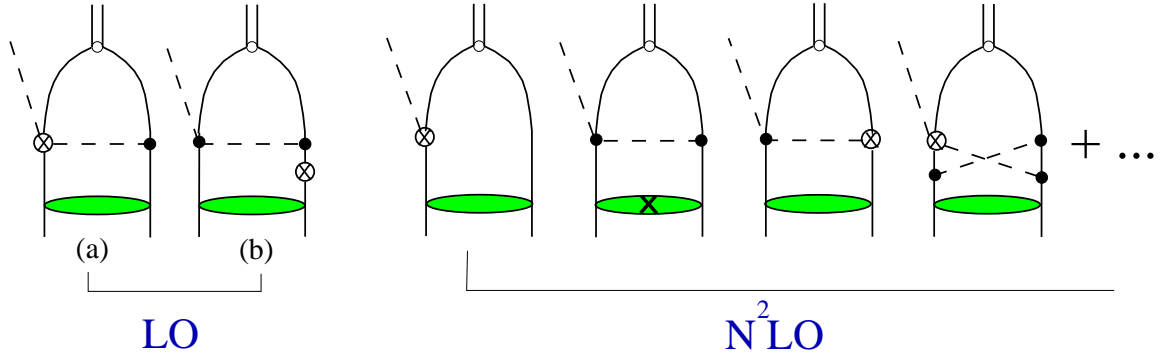


Fig. 6. Diagrams contributing to isospin violating s-wave pion production up to N<sup>2</sup>LO.

$$\mathcal{M}_{pn \rightarrow d\pi^0}^{IV,s} = M^{IV,s} \mathcal{I}(\hat{p}\varepsilon) \quad (4)$$

where  $\varepsilon$  is the deuteron polarization vector,  $\mathbf{k}_\pi$  ( $\mathbf{p}$ ) is the momentum of the pion (initial nucleon),  $\hat{k}_\pi = \mathbf{k}_\pi/k_\pi$  ( $\hat{p} = \mathbf{p}/p$ ),  $\mathcal{I} = \chi_2^T \frac{\sigma_2}{\sqrt{2}} \chi_1$  and the  $\chi$ 's stand for spinors of the initial nucleons. Here,  $M_1^{IC,p}$  and  $M_2^{IC,p}$  are the invariant amplitudes corresponding to the isospin conserving  $p$ -wave pion production in the  ${}^1S_0 \rightarrow {}^3S_1 p$  and  ${}^1D_2 \rightarrow {}^3S_1 p$  partial waves and  $M^{IV,s}$  is the corresponding amplitude for the isospin violating  $s$ -wave production in the  ${}^1P_1 \rightarrow {}^3S_1 s$  partial wave. Thus, in the latter amplitude the isovector pion is produced from an isoscalar  $NN$  pair ( $I_i = 0$ ). The expression for  $A_1$  reads

$$A_1 = \frac{1}{128\pi^2} \frac{\eta M_\pi}{p(M_\pi + m_d)^2} \text{Re} \left[ \left( M_1^{IC,p} + \frac{2}{3} M_2^{IC,p} \right) M^{IV,s} \right] \quad (5)$$

where  $m_d$  is the deuteron mass. The isospin conserving  $p$ -wave amplitudes are taken from Ref. [27]. It turns out that the contribution  $M_1^{IC,p}$  is quite uncertain due to the presence of the contact term and negligibly small. The smallness, in particular, is due to the cancellation between the direct pion emission at LO and the contribution of the  $\Delta$ -isobar at NLO. We therefore neglect the contribution  $M_1^{IC,p}$  in this calculation. On the contrary, the contribution  $M_2^{IC,p}$  is very large due to constructive interference of the direct and the  $\Delta$  production mechanisms. Moreover, due to the strong transition  $NN \rightarrow N\Delta$ , where the final  $N\Delta$  system is in the S-wave ( ${}^1D_2 \rightarrow {}^5S_2$ ), the convolution of the pion production operator via the intermediate  $\Delta$ -isobar with the deuteron wave function is large (much larger than in case of the  ${}^1S_0$  initial state).

### 3.2 Isospin violating s-wave pion production

Now we come to the discussion of the IV  $s$ -wave amplitude. Our calculations are based on the effective chiral Lagrangian [60, 61] which reads

$$\mathcal{L}^{(0)} = N^\dagger \left[ \frac{1}{4F_\pi^2} \boldsymbol{\tau} \cdot (\dot{\boldsymbol{\pi}} \times \boldsymbol{\pi}) + \frac{g_A}{2F_\pi} \boldsymbol{\tau} \cdot \boldsymbol{\sigma} \cdot \nabla \boldsymbol{\pi} \right] N + \dots, \quad (6)$$

for the leading  $\pi N$  interaction terms relevant for our study. The leading isospin-violating terms, generated by the quark-mass difference and hard-photon contributions, are

$$\begin{aligned} \mathcal{L}_{iv}^{(0)} = & \frac{\delta m_N}{2} N^\dagger \boldsymbol{\tau}_3 N - \frac{\delta m_N^{\text{str}}}{4F_\pi^2} N^\dagger \boldsymbol{\tau} \cdot \boldsymbol{\pi} \pi_3 N \\ & - \frac{\delta m_N^{\text{em}}}{4F_\pi^2} N^\dagger (\boldsymbol{\tau}_3 \boldsymbol{\pi}^2 - \boldsymbol{\tau} \cdot \boldsymbol{\pi} \pi_3) N + \dots \end{aligned} \quad (7)$$

with  $\delta m_N = m_n - m_p = \delta m_N^{\text{str}} + \delta m_N^{\text{em}}$ . The ellipses stand for further terms which are not relevant here. In the equations above  $F_\pi$  denotes the pion decay constant in the chiral limit,  $g_A$  is the axial-vector coupling of the nucleon and  $N$  ( $\boldsymbol{\pi}$ ) corresponds to the nucleon (pion) field. More precisely, this form of the IV strong and electromagnetic operators is only correct at leading order and neglecting terms with more than two pion fields. The more generic form involves the low-energy constants (LECs)  $c_5$  and  $f_2$  (for precise definitions, see e.g. [31]).

The diagrams that contribute to the amplitude  $M^{IV,s}$  up to N<sup>2</sup>LO are shown in Fig. 6, see also Ref. [62] where loops at N<sup>2</sup>LO are discussed in more detail. At LO there are two diagrams: diagram (a) corresponds to the rescattering process in which CSB occurs explicitly in the  $\pi N$  scattering vertex due to the last two terms in Eq. (7); in diagram (b) pion rescattering proceeds via the Weinberg-Tomozawa operator (first term in Eq. (6)) which produces an additional isospin violating piece from the mass difference of neutron and proton due to its time dependence as will be discussed later in this section. Note that there is no diagrams at NLO. That is why the theoretical uncertainty of the isospin violating amplitude at LO is expected to be  $\sim M_\pi/m_N \simeq 15\%$ .

In order to understand the interplay of diagram (a) and diagram (b) of Fig. 6 it is sufficient to focus on the  $\pi N$  rescattering vertex on nucleon 1. From the pion production vertex on nucleon 2 we only keep the isospin structure, for the rest is identical for both diagrams. The relevant part of diagram (a) then reads

$$\begin{aligned} \hat{I}_{(a)} = & -i \frac{\delta m_N^{\text{str}}}{4F_\pi^2} \left( \boldsymbol{\tau}^{(1)} \cdot \boldsymbol{\tau}^{(2)} + \tau_3^{(1)} \tau_3^{(2)} \right) \\ & + i \frac{\delta m_N^{\text{em}}}{4F_\pi^2} \left( \boldsymbol{\tau}^{(1)} \cdot \boldsymbol{\tau}^{(2)} - \tau_3^{(1)} \tau_3^{(2)} \right). \end{aligned} \quad (8)$$

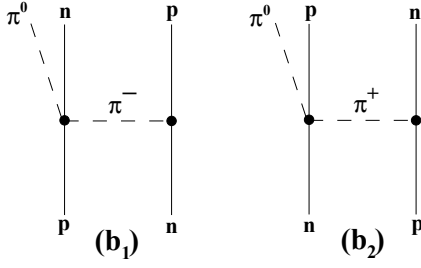


**Fig. 7.** Leading-order contributions to isospin violation due to the time-dependent Weinberg-Tomozawa operator in the particle basis.

We work at leading order in  $IV$ . Since we study an  $IV$  transition operator, we may therefore treat the external nucleons as identical particles — this is not the case for the diagram (b), where the mass difference of the external particles plays the essential role. The evaluation of the operator Eq. (8) for the isospin violating transition from the isospin zero initial  $pn$  state to the isospin zero deuteron state yields

$$\langle I_f = 0 | \hat{I}_{(a)} | I_i = 0 \rangle = \frac{i}{4F_\pi^2} 4 (\delta m_N^{\text{str}} - \delta m_N^{\text{em}}/2). \quad (9)$$

This piece represents the complete rescattering contribution included in Refs. [29, 34]. Let us now look more closely at diagram (b) of Fig. 6. The relevant part of the amplitude for this diagram can be most easily calculated in the particle basis as shown in Fig. 7. One gets

$$\langle I_f = 0 | \hat{I}_{(b)} | I_i = 0 \rangle = -\frac{1}{2} (I_{b_1} + I_{b_2}), \quad (10)$$

where  $I_{b_1}$  and  $I_{b_2}$  are the isospin coefficients corresponding to the diagrams (b<sub>1</sub>) and (b<sub>2</sub>) of Fig. 7 and the factor  $-1/2$  stems from the Clebsch-Gordan coefficients. Note that, since the WT operator involves a time derivative, the corresponding Feynman rule reads

$$V_{WT}^{ab} = \frac{1}{4F_\pi^2} \varepsilon_{abc} \tau_c (q_0 + M_\pi), \quad (11)$$

with  $a, b$  and  $c$  Cartesian pion indices and  $q_\mu$  the four-momentum of the intermediate pion. Due to the explicit appearance of  $q_0$  in  $V_{WT}$ , the final expression for diagram (b) of Fig. 6 depends on the neutron–proton mass difference. Indeed, the evaluation of this vertex for the diagrams (b<sub>1</sub>) and (b<sub>2</sub>) of Fig. 7 yields

$$V_{WT} = \frac{-i}{4F_\pi^2} \begin{cases} \sqrt{2} \left( \frac{3M_\pi}{2} + \delta m_N \right) & \text{for diagram (b}_1\text{)}, \\ -\sqrt{2} \left( \frac{3M_\pi}{2} - \delta m_N \right) & \text{for diagram (b}_2\text{)}. \end{cases} \quad (12)$$

Thus in the isospin violating contribution to Eq. (10) the terms  $\propto M_\pi$  cancel while those  $\propto \delta m_N$  survive. The non-vanishing isospin matrix element for the diagram (b) of Fig. 6 amounts to

$$\langle I_f = 0 | \hat{I}_{(b)} | I_i = 0 \rangle = -\frac{\sqrt{2}}{2} (V_{WT}^{b_1} + V_{WT}^{b_2}) = \frac{i}{4F_\pi^2} 2\delta m_N. \quad (13)$$

Adding up the contributions of diagrams (a) and (b) we find that the resulting contribution at LO depends on the quark mass contribution to the nucleon mass difference only — the electromagnetic piece vanishes completely:

$$\langle I_f = 0 | \hat{I}_{(a)} + \hat{I}_{(b)} | I_i = 0 \rangle = \frac{i}{4F_\pi^2} 6\delta m_N^{\text{str}}. \quad (14)$$

In comparison with the expression used previously (c.f. Eq. (9)) the rescattering operator gets enhanced by about 30%, when standard values  $\delta m_N^{\text{str}} = 2$  MeV and  $\delta m_N^{\text{em}} = -0.76$  MeV [30] are used.

An alternative method to derive the same result is by using the field-redefined Lagrangian as discussed in Refs. [63–65] — see also Ref. [66] where unitary transformations are used. In this formulation the pion and nucleon fields are redefined in order to eliminate the first term in the effective Lagrangian in Eq. (7). This allows one to work with nucleons as indistinguishable particles. All terms in the Lagrangian are invariant under this transformation except the ones involving a time derivative such as the Weinberg-Tomozawa operator which generates an additional isospin violating  $\pi N \rightarrow \pi N$  vertex  $\propto \delta m_N$  that cancels exactly the electromagnetic contribution to this vertex  $\propto \delta m_N^{\text{em}}$ .

For the sake of completeness, we present here the invariant amplitude  $M^{\text{IV},s}$  corresponding to the LO calculation

$$M^{\text{IV},s} = M_{\text{FSI}}^{\text{IV},s} + M_{\text{ISI+FSI}}^{\text{IV},s}, \quad (15)$$

$$M_{\text{FSI}}^{\text{IV},s}(p) = \frac{6m_N^{3/2} g_A}{F_\pi^3} \delta m_N^{\text{str}} \int \frac{d^3 p'}{(2\pi)^3} \times \left[ \left( u(p') + \frac{w(p')}{\sqrt{2}} \right) \frac{(\mathbf{p}' - \mathbf{p}) \cdot \hat{\mathbf{p}}}{(\mathbf{p}' - \mathbf{p})^2 + M_\pi^2} - \frac{3}{\sqrt{2}} w(p') \frac{((\mathbf{p}' - \mathbf{p}) \cdot \hat{\mathbf{p}})(\hat{\mathbf{p}} \cdot \hat{\mathbf{p}}')}{(\mathbf{p}' - \mathbf{p})^2 + M_\pi^2} \right], \quad (16)$$

$$M_{\text{ISI+FSI}}^{\text{IV},s} = \frac{1}{4m_N} \int \frac{d^3 q}{(2\pi)^3} \frac{M_{\text{NN}}^{\text{ISI}}(p, q) M_{\text{FSI}}^{\text{IV},s}(q)}{q^2 - p^2 - i0}, \quad (17)$$

Here  $M_{\text{NN}}^{\text{ISI}}$  is the NN invariant amplitude<sup>5</sup> corresponding to  $^1P_1$  transition in the initial state,  $u(p')$  ( $w(p')$ ) is the S-wave (D-wave) part of the deuteron wave function, normalized by the condition

$$\int \frac{d^3 p'}{(2\pi)^3} (u(p')^2 + w(p')^2) = 1. \quad (18)$$

In the calculation we use  $F_\pi = 92.4$  MeV and  $g_A = 1.32$  (utilizing the Goldberger-Treiman relation). To get the full amplitude  $M^{\text{IV},s}$  which enters the observables, we convoluted the pion production operator with  $NN$  wave functions in the initial and final states, cf. Appendix A of Ref. [27] for a detailed description. Ideally, one should use wave

<sup>5</sup> Its normalization is chosen such that in the CM frame, the amplitude  $M_{NN}$  evaluated on the energy shell is related to the scattering phase shift  $\delta(k)$  through  $M_{NN}(k, k, k^2/m_N) = 16\pi m_N(k \cot \delta(k) - ik)^{-1}$ .

functions derived in the same framework, namely ChPT. However, up to now these are only available for energies below the pion production threshold [5]. We therefore adopt the so-called hybrid approach, first introduced by Weinberg [6], i.e. we use transition operators derived within effective field theory and convolute them with realistic  $NN$  wave functions [57].

### 3.3 Results and discussion

Now we are in the position to discuss the results for the forward-backward asymmetry within the complete LO calculation. Using the values for the parameters specified above and utilizing the  $NN$  wave functions from Ref. [57], the result can be presented in the form

$$A_{fb}^{LO} = (11.5 \pm 3.5) \times 10^{-4} \frac{\delta m_N^{str}}{\text{MeV}}. \quad (19)$$

As discussed above, the calculation of the isospin violating amplitude has a theoretical uncertainty of 15% which is doubled to provide a more conservative estimate of the forward-backward asymmetry. This uncertainty is given in the expression above. The estimation includes small theoretical uncertainty of the p-wave amplitudes calculated at  $N^2LO$  and small experimental uncertainty of the total cross section.

Using the experimental result for  $A_{fb}$  [28]

$$A_{fb} = [17.2 \pm 8(\text{stat.}) \pm 5.5(\text{sys.})] \times 10^{-4} \quad (20)$$

we extract  $\delta m_N^{str}$

$$\delta m_N^{str} = (1.5 \pm 0.8 (\text{exp.}) \pm 0.5 (\text{th.})) \text{ MeV}, \quad (21)$$

where we added the experimental errors in quadrature. At the present stage, the uncertainty in the determination of  $\delta m_N^{str}$  is dominated by the experimental uncertainty for  $A_{fb}$ . This number reveals a very good agreement with the value for the same quantity extracted from the Cottingham sum rule [67] by Gasser and Leutwyler [30]

$$\delta m_N^{str} = 2.0 \pm 0.3 \text{ MeV}. \quad (22)$$

This value is also consistent with a recent determination of  $\delta m_N^{str}$  using lattice QCD [68]  $\delta m_N^{str} = 2.26 \pm 0.57 \pm 0.42 \pm 0.10$  MeV, where the uncertainties emerge from statistics, the input as well as the chiral extrapolation.

Let us now compare our results with the other theoretical investigations [29, 34] of CSB in this reaction.

First of all, we found an additional IV contribution at LO, as described in the previous section, which provides a 30% correction to the s-wave IV amplitude. Besides this, there are other reasons why our result deviates from those of Refs. [29, 34] already at leading order. The numerical evaluation of the diagram (a) of Fig. 6 revealed that the value we obtain is significantly smaller than the one found in Ref. [29]. It turned out that the result of Ref. [29] is too large by a factor of 4 due to an error. The discrepancy of our result to that of Ref. [34] after including an additional IV term at LO in Ref. [34], is an accumulation of

various effects. First of all, in Ref. [34] the isospin conserving  $s$ - and  $p$ -wave amplitudes are calculated within ChPT up to NLO. Thus, they come with individual uncertainties of 30 % and 15 %, respectively — the uncertainty for the  $s$ -wave appears doubled for this amplitude, since it enters squared in  $A_0$ , while the  $p$ -wave amplitudes mainly contribute linearly to  $A_1$  — c.f. Eq. (5). In contrast to this we take the  $s$ -wave amplitude directly from data, with a negligible uncertainty and for the  $p$ -wave amplitudes the results of Ref. [27] outlined above, which were calculated to NNLO and are additionally constrained by data. Thus, combining these uncertainties with that for the CSB amplitude in quadrature, a total uncertainty of 50 % arises for the result of Ref. [34]. In addition, as explained in Sec. 3.1, the IC p-wave pion amplitudes get an important contribution from the  $\Delta$  isobar in the intermediate state. To have this contribution under control we use a coupled channel approach [57] that includes  $NN$  and  $N\Delta$  channels explicitly. However, in Ref. [34] the  $N\Delta$  potential is added on top of the existing  $NN$  model and therefore the strength of the corresponding  $NN \rightarrow N\Delta$  transition potential is not constrained by the NN phase shifts. To put some constraints on this transition a phenomenological formfactor was introduced in Ref. [34] where the cut-off  $\Lambda \simeq 400$  MeV was chosen to obtain the best fit to experimental data in pion production. However, the analyzing power, which is linear with the p-wave amplitudes, is still off the data by about 30% in the relevant region. These effects together — the larger uncertainty of the calculation of Ref. [34] as well as differences in the  $p$ -wave amplitudes — basically explain the discrepancy between our result and that of Ref. [34].

## 4 Summary

We have discussed the results of a recent calculation [27] for the  $p$ -wave pion production amplitudes in  $NN$  collisions in three different channels ( $pn \rightarrow pp\pi^-$ ,  $pp \rightarrow d\pi^+$  and  $pp \rightarrow pn\pi^+$ ) in the framework of chiral effective field theory. It was demonstrated that the experimental observables in all these channels can be simultaneously described by adjusting only one low-energy constant contributing at  $N^2LO$ . Furthermore, it is found that the net contribution of the diagrams at  $N^2LO$  is indeed of the size predicted by the power counting. These results demonstrate the validity of the employed approach to the pion production reactions characterized with the large momentum transfer.

Based on the progress in understanding of the isospin conserving pion production we have investigated charge symmetry breaking effects in  $pn \rightarrow d\pi^0$ . In this reaction CSB effects manifest themselves in the forward-backward asymmetry of the differential cross section. We performed a complete calculation of this asymmetry at leading order. We showed that the resulting production operator is driven by that contribution to the neutron-proton mass difference which is coming solely from the quark mass difference,  $\delta m_N^{str}$ . Using the TRIUMF measurement of the forward-backward asymmetry [28] we extracted

$$\delta m_N^{str} = 1.5 \pm 0.9 \text{ MeV}, \quad (23)$$

This number is in good agreement with the results of Gasser and Leutwyler based on the Cottingham sum rule and with the results of lattice QCD. At present the uncertainty in our analysis of  $\delta m_N^{\text{sr}}$  is dominated by the experimental error bars – an improvement on this side would be very important. On the other hand, a calculation of loops at N<sup>2</sup>LO is also called for to confirm the theoretical uncertainty estimate. Also the investigation of the isospin violating reaction  $dd \rightarrow \alpha\pi^0$  where the experimental data exist due to the measurement at TRIUMF [69] could be very helpful to constrain the LEC contributing at N<sup>2</sup>LO to  $pn \rightarrow d\pi^0$ . First attempts to study this reaction are made in Refs. [62, 70–72]

#### Acknowledgments

I would like to thank E. Epelbaum, A. Filin, J. Haidenbauer, C. Hanhart, A. Kudryavtsev, V. Lensky and U.-G. Meißner for fruitful collaboration the results of which were presented in this Conference. I thank the organizers for the well-organized conference and for the invitation to give this talk. Work supported in parts by funds provided from the Helmholtz Association (grants VH-NG-222, VH-VI-231) and by the DFG (SFB/TR 16 and DFG-RFBR grant 436 RUS 113/991/0-1) and the EU HadronPhysics2 project. I acknowledge the support of the State Corporation of Russian Federation “Rosatom”.

#### References

1. S. Weinberg, *Physica A* **96**, (1979) 327.
2. J. Gasser and H. Leutwyler. *Ann. Phys.* **158**, (1984) 142.
3. G. Colangelo, J. Gasser and H. Leutwyler, *Nucl. Phys. B* **603**, (2001) 125 [arXiv:hep-ph/0103088].
4. V. Bernard and U.-G. Meißner, *Ann. Rev. Nucl. Part. Sci.* **57**, (2007) 33 [arXiv:hep-ph/0611231].
5. P. F. Bedaque and U. van Kolck, *Ann. Rev. Nucl. Part. Sci.* **52**, (2002) 339; [arXiv:nucl-th/0203055]; E. Epelbaum, *Prog. Part. Nucl. Phys.* **57**, (2006) 654; [arXiv:nucl-th/0509032]; E. Epelbaum, H.-W. Hammer and U.-G. Meißner, arXiv:0811.1338 [nucl-th], *Rev. Mod. Phys.*, in print.
6. S. Weinberg, *Phys. Lett. B* **295**, (1992) 114.
7. J. Gasser, V. E. Lyubovitskij and A. Rusetsky, *Phys. Rept.* **456**, (2008) 167 [arXiv:0711.3522 [hep-ph]]; U.-G. Meißner, U. Raha and A. Rusetsky, *Eur. Phys. J. C* **41**, (2005) 213; *Phys. Lett. B* **639**, (2006) 478
8. S. R. Beane, V. Bernard, E. Epelbaum, U.-G. Meißner and D. R. Phillips, *Nucl. Phys. A* **720**, (2003) 399 [arXiv:hep-ph/0206219].
9. V. Baru et al., *In the Proceedings of MENU 2007, Julich, Germany, 10-14 Sep 2007, pp 127* [arXiv:0711.2743 [nucl-th]]; V. Baru, J. Haidenbauer, C. Hanhart, A. E. Kudryavtsev, V. Lensky and U.-G. Meißner, *Phys. Lett. B* **659**, (2008) 184 [arXiv:0706.4023 [nucl-th]]; V. Lensky, V. Baru, J. Haidenbauer, C. Hanhart, A. E. Kudryavtsev and U.-G. Meißner, *Phys. Lett. B* **648**, (2007) 46 [arXiv:nucl-th/0608042].
10. V. Baru, J. Haidenbauer, C. Hanhart and J. A. Niskanen, *Eur. Phys. J. A* **16**, (2003) 437 [arXiv:nucl-th/0207040].
11. A. Gårdestig and D. R. Phillips, *Phys. Rev. C* **73**, (2006) 014002 [arXiv:nucl-th/0501049].
12. A. Gårdestig, *Phys. Rev. C* **74**, (2006) 017001 [arXiv:nucl-th/0604035].
13. V. Lensky et al., *Eur. Phys. J. A* **26**, (2005) 107 [arXiv:nucl-th/0505039].
14. V. Lensky et al., *Eur. Phys. J. A* **33**, (2007) 339 [arXiv:0704.0443 [nucl-th]].
15. S. R. Beane, V. Bernard, T. S. H. Lee, U.-G. Meißner and U. van Kolck, *Nucl. Phys. A* **618**, (1997) 381 [arXiv:hep-ph/9702226].
16. H. Krebs, V. Bernard and U.-G. Meißner, *Eur. Phys. J. A* **22**, (2004) 503 [arXiv:nucl-th/0405006].
17. B.Y. Park et al., *Phys. Rev. C* **53**, (1996) 1519.
18. C. Hanhart, J. Haidenbauer, M. Hoffmann, U.-G. Meißner and J. Speth, *Phys. Lett. B* **424**, (1998) 8.
19. V. Bernard, N. Kaiser and U.-G. Meißner, *Eur. Phys. J. A* **4**, (1999) 259.
20. T.D. Cohen et al., *Phys. Rev. C* **53**, (1996) 2661 [arXiv:nucl-th/9512036].
21. C. da Rocha, G. Miller and U. van Kolck, *Phys. Rev. C* **61**, (2000) 034613 [arXiv:nucl-th/9904031].
22. C. Hanhart, U. van Kolck, and G.A. Miller, *Phys. Rev. Lett.* **85**, (2000) 2905 [arXiv:nucl-th/0004033].
23. C. Hanhart and N. Kaiser, *Phys. Rev. C* **66**, (2002) 054005 [arXiv:nucl-th/0208050].
24. C. Hanhart, *Phys. Rept.* **397**, (2004) 155 [arXiv:hep-ph/0311341].
25. V. Lensky, et al., *Eur. Phys. J. A* **27**, (2006) 37, [arXiv:nucl-th/0511054].
26. Y. Kim et al., *Phys. Rev. C* **80**, (2009) 015206 [arXiv:0810.2774 [nucl-th]].
27. V. Baru, E. Epelbaum, J. Haidenbauer, C. Hanhart, A. E. Kudryavtsev, V. Lensky and U.-G. Meißner, *Phys. Rev. C* **80**, (2009) 044003 [arXiv:0907.3911 [nucl-th]].
28. A. K. Opper *et al.*, *Phys. Rev. Lett.* **91**, (2003) 212302 [arXiv:nucl-ex/0306027].
29. U. van Kolck, J. A. Niskanen and G. A. Miller, *Phys. Lett. B* **493**, (2000) 65 [arXiv:nucl-th/0006042].
30. J. Gasser and H. Leutwyler, *Phys. Rept.* **87**, (1982) 77.
31. U.-G. Meißner and S. Steininger, *Phys. Lett. B* **419**, (1998) 403.
32. N. Fettes, U.-G. Meißner and S. Steininger, *Phys. Lett. B* **451**, (1999) 233; N. Fettes and U.-G. Meißner, *Phys. Rev. C* **63**, (2001) 045201; N. Fettes and U.-G. Meißner, *Nucl. Phys. A* **693**, (2001) 693; M. Hoferichter, B. Kubis and U.-G. Meißner, *Phys. Lett. B* **678**, (2009) 65.
33. A. Filin, V. Baru, E. Epelbaum, J. Haidenbauer, C. Hanhart, A. Kudryavtsev and U.-G. Meißner, *Phys. Lett. B* **681**, (2009) 423 [arXiv:0907.4671 [nucl-th]].
34. D. R. Bolton and G. A. Miller, arXiv:0907.0254 [nucl-th].
35. E. Epelbaum et al., *Phys. Rev. C* **66**, (2002) 064001 [arXiv:nucl-th/0208023].

36. T. S. Park *et al.*, Phys. Rev. C **67**, (2003) 055206.
37. A. Gårdestig and D. R. Phillips, Phys. Rev. Lett. **96**, (2006) 232301.
38. D. Gazit, S. Quaglioni and P. Navratil, Phys. Rev. Lett. **103**, (2009) 102502 [arXiv:0812.4444 [nucl-th]].
39. S. X. Nakamura, Phys. Rev. C **77**, (2008) 054001.
40. M. Goldberger and K.M. Watson, *Collision Theory* (Wiley, New York, 1964).
41. R. Omnès, Nuovo Cim. **8**, (1958) 316.
42. A. Gasparyan, J. Haidenbauer, C. Hanhart and J. Speth, Phys. Rev. C **69**, (2004) 034006; A. Gasparyan, J. Haidenbauer and C. Hanhart, Phys. Rev. C **72**, (2005) 034006.
43. B. G. Ritchie *et al.*, Phys. Rev. C **47**, (1993) 21.
44. P. Heimberg *et al.*, Phys. Rev. Lett. **77**, (1996) 1012.
45. M. Drochner *et al.* [GEM Collaboration], Nucl. Phys. A **643**, (1998) 55.
46. E. Korkmaz *et al.*, Nucl. Phys. A **535**, (1991) 637.
47. E. L. Mathie *et al.*, Nucl. Phys. A **397**, (1983) 469.
48. A. Kacharava *et al.*, “Spin physics from COSY to FAIR,” arXiv:nucl-ex/0511028.
49. H. Hahn *et al.*, Phys. Rev. Lett. **82**, (1999) 2258.
50. F. Duncan *et al.*, Phys. Rev. Lett. **80**, (1998) 4390.
51. M. Daum *et al.*, Eur. Phys. J. C **25**, (2002) 55.
52. R. Bilger *et al.*, Nucl. Phys. A **693**, (2001) 633.
53. H.O. Meyer *et al.*, Phys. Rev. Lett. **83**, (1999) 5439; Phys. Rev. C **63**, (2001) 064002.
54. P. N. Deepak, J. Haidenbauer and C. Hanhart, Phys. Rev. C **72**, (2005) 024004.
55. R.W. Flammang *et al.*, Phys. Rev. C **58**, (1998) 916.
56. J. A. Niskanen, Nucl. Phys. A **298**, (1978) 417.
57. J. Haidenbauer, K. Holinde and M. B. Johnson, Phys. Rev. C **48**, (1993) 2190.
58. V. Baru *et al.*, Proceedings of MENU 2007, Jülich, Germany, 10-14 Sep 2007, pp 128 [arXiv:0711.2748 [nucl-th]].
59. P. Hauser *et al.*, Phys. Rev. C **58**, (1998) 1869; Th. Strauch *et al.*, In Proceedings of EXA08, September 2008, Vienna, Austria, published in Hyperfine Interactions; Th. Strauch, PhD thesis, Cologne, 2009; see also talk given in this Conference.
60. C. Ordóñez, L. Ray, and U. van Kolck, Phys. Rev. Lett. **72**, 1982 (1994); Phys. Rev. C **53**, (1996) 2086.
61. V. Bernard, N. Kaiser and U.-G. Meißner, Int. J. Mod. Phys. E **4** (1995) 193.
62. A. Gårdestig *et al.*, Phys. Rev. C **69**, (2004) 044606.
63. J. L. Friar *et al.*, Phys. Rev. C **70**, (2004) 044001.
64. J. L. Friar, G. L. Payne and U. van Kolck, Phys. Rev. C **71**, (2005) 024003.
65. E. Epelbaum, H. Krebs and U.-G. Meißner, Nucl. Phys. A **806**, (2008) 65.
66. E. Epelbaum, U.-G. Meißner and J. E. Palomar, Phys. Rev. C **71**, (2005) 024001; E. Epelbaum and U.-G. Meißner, Phys. Rev. C **72**, (2005) 044001.
67. W.N. Cottingham, Ann. Phys. **25**, (1963) 424.
68. S. R. Beane, K. Orginos and M. J. Savage, Nucl. Phys. B **768**, (2007) 38.
69. E. J. Stephenson *et al.*, Phys. Rev. Lett. **91**, (2003) 142302.
70. A. Nogga *et al.*, Phys. Lett. B **639**, (2006) 465.
71. T. A. Lahde and G. A. Miller, Phys. Rev. C **75**, (2007) 055204 [Erratum-ibid. C **77**, (2008) 019904].
72. A. C. Fonseca, R. Machleidt and G. A. Miller, arXiv:0907.0215 [nucl-th].